Development of Covalent Organic Polymer as a Photocatalyst

M.Sc. Thesis

by

Mithu Roy

DISCIPLINE OF CHEMISTRY

INDIAN INSTITUTE OF TECHNOLOGY INDORE

JUNE, 2019

Development of Covalent Organic Polymer as a Photocatalyst

A Thesis

Submitted in partial fulfillment of the requirements for the award of the degree
of
Master of Science

by
Mithu Roy

DISCIPLINE OF CHEMISTRY
INDIAN INSTITUTE OF TECHNOLOGY INDORE
JUNE, 2019

INDIAN INSTITUTE OF TECHNOLOGY INDORE

CANDIDATE'S DECLARATION

I hereby certify that the work which is being presented in the thesis entitled **Development of Covalent Organic Polymer as a Photocatalyst** in the partial fulfilment of the requirements for the award of the degree of **Master of Science** and submitted in the **Discipline of Chemistry, Indian Institute of Technology Indore**, is an authentic record of my own work carried out during the time period from **July 2018** to **June 2019** under the supervision of **Dr. Apurba K. Das**, Associate Professor, Discipline of Chemistry, IIT Indore.

The matter presented in this thesis has not been submitted by me for the award of any other degree of this or any other institute.

Mithu Roy

This is to certify that the above statement made by the candidate is correct to the best of my/our knowledge.

Dr. Apurba K. Das

MITHU ROY has successfully given his/her M.Sc. Oral Examination held on **01/07/2019**

Signature of Supervisor of MSc thesis
Date:

Convener, DPGC
Date:

Signature of PSPC Member
Date:

Signature of PSPC Member
Date:

Acknowledgments

I would like to thanks my project supervisor **Dr. Apurba K. Das** (Associate Professor, Discipline of chemistry, IIT Indore) for allowing me to work in the field of my interest with his research group. His valuable guidance, advice, and motivational support throughout the project work help me to complete my project work.

I would also like to thanks **Dr. Anjan Chakraborty** and **Dr. Tushar Kanti Mukherjee** for their valuable suggestions and guidance.

I wish to express my gratitude to **Prof. Pradeep Mathur**, Director, IIT Indore, for his continuous encouragement, help, and support in every aspect.

I would like to thank all the faculty members of the Discipline of Chemistry for their motivational inspiration.

I would also like to thank all of the lab-members for their valuable suggestion and help. Without their support; this report would not be possible.

I would like to thank the Discipline of Chemistry, IIT Indore for allowing me to work in the laboratory.

I am also thankful to SIC, IIT Indore and its member for their technical help and support.

I am also thankful to all my friends, who helped me directly-indirectly during my post-graduation program.

I would also like to express my deepest gratitude to my family and friends for their kind cooperation, understanding, and valuable support.

Mithu Roy

M.Sc. 2nd year

Roll No.-1703131012

Discipline of Chemistry

IIT Indore

Dedicated to My Family

Abstract

The conjugated ene-yne based on covalent organic polymers (COPs) have been taken great attention in the research field to rectify environmental issues. Herein we have synthesized a peptide functionalized diacetylene based compound. The compound which we have synthesized in this project undergoes self-assemblies to form organogel and also undergoes topochemical photopolymerization upon UV light irradiation forming a one-dimensional conjugated ene-yne based nanofibers like covalent organic polymer (COP) nanostructures, which shows substantial recyclable photocatalytic activity for the disintegration of dye. Upon UV light treatment, 89% of the rhodamine b dye disintegration was observed in the presence of COP as a photocatalyst after 120 minutes. The covalent organic polymer was found to be highly stable, and there was no significant weight loss observed after several photocatalytic reactions. The stability of the photocatalyst was explained from the FT-IR spectrum. These stable and cheap polymer nanofibers are easy to synthesize and can be reused without any noticeable loss of activity.

TABLE OF CONTENTS

LIST OF FIGURES

LIST OF TABLES

NOMENCLATURE

nm	Nanometer
δ	Delta
µm	Micrometer
µM	Micro molar
mL	Milliliter
mg	Milligram
g	Gram
ʎ	Lambda

ACRONYMS

Abbreviations used for compounds, substituents, reagents, etc. are mainly by the recommendations of the IUPAC. Additional abbreviations used in this thesis are listed below.

F	Phenylalanine
F-OMe	Phenylalanine methyl ester
$CDCl_3$	Chloroform d
DMSO d_6	Dimethyl Sulfoxide d6
DMF	*N*, *N*-Dimethylformamide
HCl	Hydrochloric acid
Na_2CO_3	Sodium Carbonate
aq.	Aqueous
d	Doublets
EtOAc	Ethyl Acetate
ESI-MS	Electron Ionization Mass Spectrometry
NaOH	Sodium Hydroxide
MeOH	Methanol
NMR	Nuclear Magnetic Resonance
s	Singlet
min.	Minute
$SOCl_2$	Thionyl chloride
TLC	Thin Layer Chromatography
t	Triplet

UV-Vis	UV- Visible
ACN	Acetonitrile
DCC	Diisopropylcarbodiimide
HOBt	N-Hydroxy benzotriazole
Na_2SO_4	Sodium sulphate
EDC.HCl	1-(3-dimethylaminopropyl)-3-ethylcarbodiimide hydrochloride
DMAP	4-dimethylaminopyridine
$TBAPF_6$	Tetrabutylammonium hexafluorophosphate

Chapter 1: Introduction and Reaction Scheme

1.1 Introduction

Water plays an essential role to maintain our daily life and for a healthy society. Now a day's water contamination becomes a major factor behalf of the fast expansion of populations and the reckless evolution of industries. Water contaminated through numerous sources, among them, the soluble organic dyes play a vital role in the contamination of water[1]. Since we are not able to resolve the environmental issues immediately, but we can reduce the water contamination by using several approaches, one of them is photocatalytic disintegration of dye. The increased amount of industrial dye contaminated water executed important threats on water safety, which can be treated with by innovative ideas**.** In the last few decades, research on diacetylene motifs plays considerable attention. Wegner has reported the first polydiacetylene (PDA) compound at around 1960s[2] because of the colourful feature of these compounds scientists are very much interested in working on these compounds. Diacetylene containing compounds due to their versatile utility becomes a significant research area. The diacetylene containing covalent organic polymers (COPs) were potentially used in semiconducting fibrous, catalysis, separation and storage of gas, sensing, optoelectronics, energy storage, and degradation of harmful dyes[3-7]. Photocatalytic dye degradation helps to reduce water contamination some extent, and it is indirectly contributing to making a green environment. Oxide-containing Semiconductors like TiO_2, ZnO, Fe_2O_3, and sulfide containing semiconductors like CdS, and ZnS were largely used as good photocatalysts.[8–13] The photocatalytic activity of these semiconductors can be enhanced in the visible region by adding some modifier like metal nanoparticles.[14–21] However the modified semiconductor photocatalysts are not suitable due to their high cost and toxicity. Alternatively, researchers are looking for cheap and green photocatalyst. Like metal-semiconductor, MOFs and COPs are also exhibited photocatalytic activity under both in UV and visible light.[22,23] There are some Metal-organic frameworks reported which degrade harmful Rhodamine 6G and methyl orange dye upon visible light treatment.[17,24-27]

The conditions for the photopolymerization of monomeric diacetylenes are the distance between two diyne axis are 4.9 Å, and the angle between the two diyne axis is 45°. The photopolymerization undergoes through 1,4-addition upon the treatment of UV light (254 nm). For the polymerization, there was no requirement of any additional catalyst; therefore, the formation of by-product is not possible, and it is happening at the room temperature. The COP formed has a core structure of ene-yne conjugation, and due to the prolonged π- conjugation the COP has the intense red colour (λ_{max} = 527 nm) and also shows the excellent optical and electronic properties.

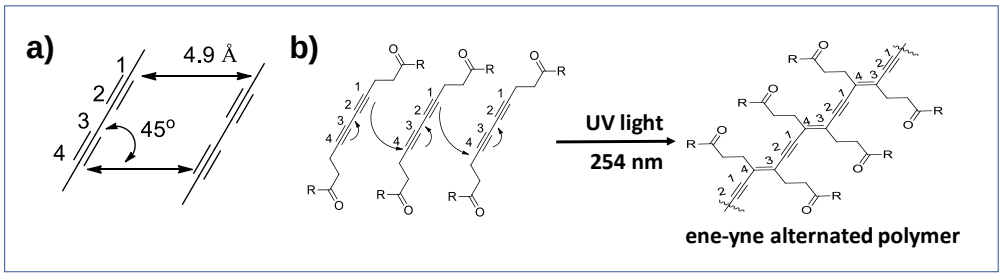

Figure 1. a) The angle and distance between two diyne axis**,** b) Schematic representation of photopolymerization.

To keep in mind, the significance of the degradation of harmful dye by using the photocatalytic method, peptide-containing diacetylene based compound was synthesized, and it is converted into the polymeric form (COP) by the treatment of UV light. The compound after photopolymerization gives a stable nanofibrous network of peptide-containing conjugated ene-yne based covalent organic polymer. The activity of the COP as a Photocatalyst was studied by the photocatalytic disintegration of rhodamine b dye upon the treatment of UV light. Herein we are reporting a new and different kind of peptide-containing conjugated ene-yne based covalent organic polymer which shows a significant amount of photocatalytic activity towards the degradation of organic pollutant like rhodamine b dye upon the treatment of UV light.

1.2 Reaction Scheme

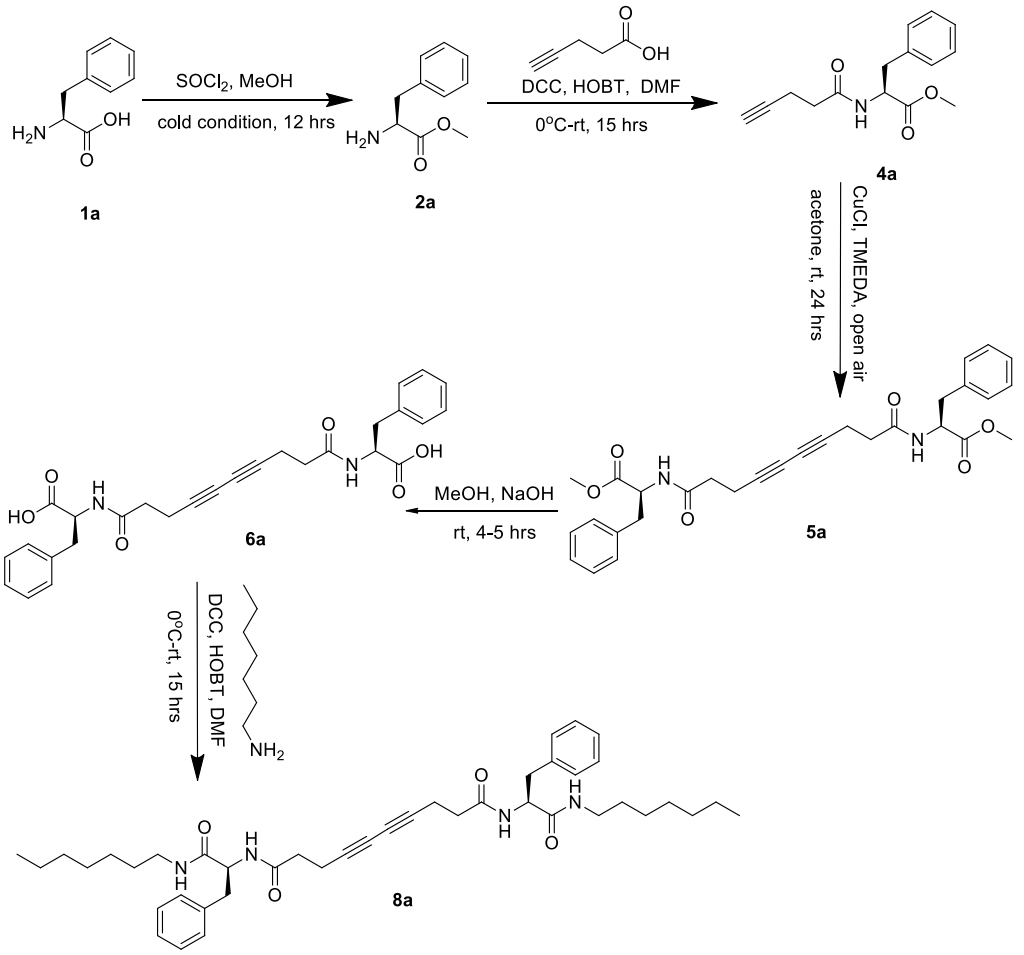

Chapter 2: Experimental sections

2.1 Materials

4-Pentynoic acid, CuCl (copper(I) chloride) and N, N, N, N-tetramethyl ethylenediamine (TMEDA) were bought from Alfa Aesar India. L-Phenylalanine, HOBt (1-hydroxybenzotriazole), DCC (N, N-dicyclohexylcarbodiimide), EDC.HCl (1-(3-dimethylaminopropyl)-3-ethyl carbodiimide hydrochloride) and DMAP (4-dimethylaminopyridine) were obtained commercially. To carry out the reactions and purification of the compounds, the solvents were distilled by following the reported literature procedures. The reactions were monitored by thin-layer chromatography (TLC). All the intermediates and final compounds were purified and characterized by using ^{1}H NMR (400 MHz) spectroscopy and mass spectrometry.

2.2 General

Mass spectrometry was done on a Bruker MicrOTOF-Q II by positive mode electrospray ionization. NMR spectroscopy was carried out on a Bruker AV 400 MHz spectrometer at 298 K. The FT-IR spectra of all the reported compounds were performed on a Bruker (Tensor-27) FT-IR spectrometer. Raman study was executed by using a Micro Raman system from Jobin Yvon Horiba LABRAM-HR visible (400-1100 nm) equipped with an Ar^{+} laser (488 nm, 10 mW) excitation source and CCD detector.

2.3 Synthesis of Compounds

2.3.1 Synthesis of methyl ester of phenylalanine: In a 100 mL round bottom flask 25 mL MeOH was taken and stirred for 15 minutes in cold condition. Then thionyl chloride (2 equiv) was added via dropping funnel to the cold solution. Finally, phenylalanine was added to the pre-cooled reaction mixture, and a guard tube was fitted with the round bottom flask. The reaction mixture was stirred for 12 hours at room temperature, and the solvent was evaporated. The crude product was washed with diethyl ether.

2.3.2 Synthesis of compound 4a: 4-pentynoic acid (1 equiv) was taken in a 100 mL round bottom flask and dissolved in 5 mL of dry DMF. The solution

was stirred for 10 minutes in cold condition, and then DCC (1.2 equiv) was added, followed by HOBt (1.2 equiv). Methyl ester protected amino acid was isolated from its corresponding methyl ester hydrochloride (2.0 eqiv) by neutralization and subsequently extracted twice with ethyl acetate (2 × 25 mL). The collected ethyl acetate extracts were dried over anhydrous Na_2SO_4 and concentrated to 3 mL. The concentrated solution was then added to the pre-cooled reaction mixture, and the reaction mixture was stirred for 12 hours. After completing, the reaction, dicyclohexylurea (DCU) was filtered off. The organic residue was washed by 1 N HCl (20 mL × 3) followed by Na_2CO_3 (20 mL × 3) and brine (20 mL × 3). Then the organic residue was dried over anhydrous Na_2SO_4 and evaporated in vacuum. Finally, the product obtained was purified by using flash column chromatography (200-400 mesh) using hexane-ethyl acetate (7:3) as eluent. The product was fully characterized by the spectroscopic data (^{1}H NMR, ^{13}C NMR, and ESI-MS) (yield 89%, 1.1856 g). ^{1}H NMR (400 MHz) data δ(ppm) value in $CDCl_3$: (1.94, 1H, s), (2.39, 2H, t), (2.47, 2H, t), (3.10, 2H, m), (3.71, 3H, s), (4.89, 1H, s), (6.05, 1H, d), (7.09, 2H), (7.24, 3H). ^{13}C NMR (100 MHz) data δ(ppm) value in $CDCl_3$: 171.89, 170.05, 135.72, 129.31, 128.63, 127.20, 76.12, 66.12, 53.18, 52.40, 37.88, 34.86, 15.46.

2.3.3 Synthesis of compound 5a: In a 100 mL round bottom flask 5 mL of dry acetone was taken and CuCl (copper(I)chloride) (2 equiv) followed by TMEDA (2 equiv) was added. The reaction mixture was stirred for 30 minutes, and then the compound **4a** (1 equiv) was added. The reaction mixture was kept for 24 hours at open air condition. After completing the reaction, the solvent was evaporated in vacuum, and the residue was dissolved in ethyl acetate. Then the ethyl acetate part was washed with 1 N HCl (30 mL × 1) and concentrated by rotary evaporation to get the crude product. The crude product was purified by using silica gel column chromatography (100-200 mesh) using hexane-ethyl acetate (5:5) as eluent. The product was fully characterized by the spectroscopic data (^{1}H NMR, ^{13}C NMR, and ESI-MS) (yield 39% 0.3491 g). ^{1}H NMR (400 MHz) data δ(ppm) value in $CDCl_3$: (2.34, 4H, t), (2.54, 4H, t), (3.10, 4H, d), (3.70, 6H, s), (4.85, 2H, d), (5.97, 2H, d), (7.07, 4H), (7.23, 6H). ^{13}C NMR (100 MHz) data δ(ppm) value in $CDCl_3$: 171.96, 170.45, 135.76, 129.31, 128.61, 127.18, 82.76, 69.42, 53.15, 52.38, 37.89, 35.17, 14.68.

2.3.4 Synthesis of compound 6a: In a 100 mL round bottom flask 1 g of compound **4a** was dissolved in 20 mL MeOH, and 2 mL of 1 N NaOH was added dropwise. The reaction mixture was stirred for 4-5 hours, and the reaction was monitored by thin layer chromatography (TLC). After completing the reaction, the solvent was evaporated, and the residue was dissolved in 30 mL water. The aqueous part of the reaction mixture was washed with diethyl ether (2 × 10 mL), then cooled in an ice water bath for 10 minutes and the Ph was adjusted to acidic Ph upon the dropwise addition of 1 N HCl. It was extracted with ethyl acetate (3 × 40 mL), and then the ethyl acetate layer was dried over anhydrous Na_2SO_4 and evaporated under vacuum to yield the corresponding carboxylic acid, which was used for the next step without any further purification. The compound was characterized by ^{1}H NMR, ^{13}C NMR, and ESI-MS data. ^{1}H NMR (400 MHz) data ẟ(ppm) value in DMSO-d_6: (2.29, 4H, t), (2.40, 4H, t), (2.88, 2H, d), (3.06, 2H, d), (4.42, 2H, d), (7.22, 10H), (8.24, 2H, d), (12.64, 2H, bs). ^{13}C NMR (100 MHz) data ẟ(ppm) value in DMSO-d_6:173.41, 170.47, 138.01, 129.58, 128.67, 126.90, 77.77, 65.79, 53.93, 37.31, 33.90, 15.16.

2.3.5 Synthesis of compound 8a: In a 100 mL round bottom flask compound **6a** (1 equiv) was dissolved in 5 mL of dry DMF. The solution was stirred for 15 minutes in ice-cold condition, and then HOBT (1 equiv) was added, followed by EDC.HCl (1.1 equiv). After that, 1-heptylamine (1.5 equiv) was added to the precooled reaction mixture followed by DMAP (4-dimethylaminopyridine) (0.05 equiv), and the reaction mixture was stirred for 12 hours. After completion of the reaction, the solvent was evaporated, and the residue was dissolved in chloroform. The organic residue was washed by 1 N HCl (20 mL × 3) followed by Na_2CO_3 (20 mL × 3) and brine (20 mL × 3). Then the organic residue was dried over anhydrous Na_2SO_4 and evaporated in vacuum. The purification of the crude product was done by using silica gel column chromatography (100-200 mesh) using chloroform-methanol (9.5:0.5) as eluent. The product was fully characterized by the spectroscopic data (^{1}H NMR, ^{13}C NMR, and ESI-MS) (yield 39% 0.3491 g). ^{1}H NMR (400 MHz) data ẟ(ppm) value in DMSO-d_6: (0.86, 6H, t), (1.29, 20H, m), (2.29, 4H, t), (2.35, 4H, t), (2.75, 2H, d), (2.91, 6H, m), (4.46, 2H, t), (7.20, 10H, m), (7.88, 2H, t),

(8.14, 2H, d). ^{13}C NMR (100 MHz) data δ(ppm) value in DMSO-d_6: 171.07, 170.18, 138.29, 129.59, 128.47, 126.68, 77.82, 65.74, 54.48, 39.39, 39.38, 33.99, 31.71, 29.41, 28.88, 26.72, 22.53, 15.17, 14.44.

2.4 Topochemical photopolymerization procedure: Topochemical photopolymerization was performed in both solid as well as in the gel phase. In the case of the solid phase, 50 mg of powdered sample was taken in a glass slide and placed in a UV chamber and treated with 254 nm UV light by the use of a 96 W UV lamp. In the case of the gel phase polymerization, in a quartz tube, 2 mL of gel (in toluene) was prepared and treated with 254 nm UV light by the use of a 96 W UV lamp.

Chapter 3: Results and Discussion/Analysis

3.1 Gelation study of the final compounds: 13.66 mg of the gelator peptide-containing diacetylene based compound (8a) was taken in a glass vial and dissolved it in 1 mL of toluene. The mixtures were then sonicated for 30 s and followed by heating at 105 °C to solubilize the gelator molecules completely. Then the clean solution was allowed to cool at room temperature. White, opaque, self-standing organogel (**Figure 2**) was formed within 5 mins. The gelation was confirmed by vial-inversion methods. The gelation process was attributed due to the self-assembly, induced by the π-π stacking interactions, intermolecular H-bondings and hydrophobic interactions of the peptide's molecules. The gelation process was further checked in several organic solvents (**Table 1**), but no gelation was observed.

Figure 2. Organogel of the compound **8a** in toluene.

Table 1. Gelation study of the final compound **8a.**

Solvent	Observation of compound 8a (20 mmol)
Toluene	Gel
Acetonitrile	P
Cyclohexane	Sol
Tetrahydrofuran	Sol
Chloroform	Sol
Dichloromethane	Sol
1,4-dioxane	Sol

3.2 Rheology study of the gel: Rheological experiment of the gel was carried out to examine the strength of the gel. The strength of the supramolecular gel means how much strongly the gel will capture the solvent molecules inside the three-dimensional network because of that movement of the solvent molecules will stop. Dynamic frequency sweep and amplitude sweep experiments of the toluene gel of compound 8a were carried out to know the storage and loss moduli (G′ and G″). The storage modulus G′ denotes a solid-like behavior, which indicates the power of the gel to resist the

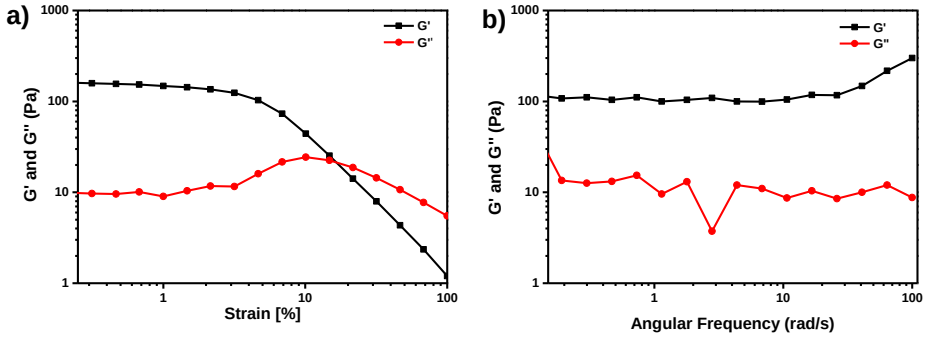

Figure 3. a) Amplitude sweep of toluene gel of compound 8a, b) Dynamic frequency sweep of toluene gel of compound 8a. Storage modulus G′ is higher than the loss modulus G″ which indicates excellent solid-like behavior of the gel materials.

deformation upon pressure. While the loss modulus G″ denotes the liquid-like character that indicates the intensity of the molecule to flow. The condition for the formation of the rigid gel is that the value of storage modulus (G′) should be higher than that of loss modulus (G″). The toluene gel of the compound **8a** shows (**Figure 3a** and **3b**) that the storage modulus (G′) is higher than the loss modulus (G″). This indicates the formation of a strong supramolecular gel.

3.3 Polymerization studies: To undergo topochemical photopolymerization, the diacetylene units have to arranged in an ordered manner. The mandatory conditions for the photopolymerization are the angle between the two diyne axis is 45^{o,} and the distance between the two diyne axis is 4.9 Å. Here we have carried out topochemical photopolymerization both in solid as well as in the gel phase. The peptide containing diacetylene monomers undergo topochemical photopolymerization through 1,4-addition to form conjugated ene-yne polymer by the treatment of ultraviolet light. After polymerization the white color of the monomer changes to red (**Figure 4a).** In the case of gel state polymerization, the gel state remains intact after ultraviolet light irradiation (**Figure 4b**). To confirm the topochemical photopolymerization UV visible spectroscopy and Raman spectroscopy was carried out.

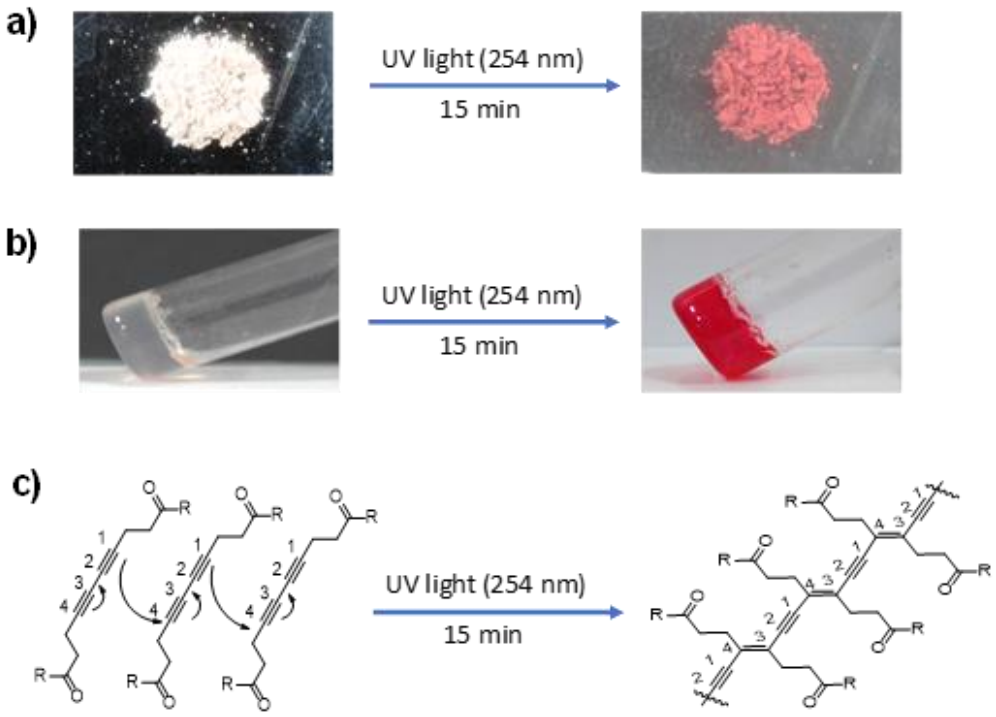

Figure 4. a) solid state photopolymerization, b) Gel phase (in toluene) photopolymerization, c) Schematic mechanism of photopolymerization.

3.4 UV visible spectroscopic studies: UV-Vis absorption spectra of compound **8a** was recorded using a Varian Cary100 Bio UV-Vis spectrophotometer. All the samples were diluted to 2 mM as concentration, and UV-Vis spectra were recorded. Before UV irradiation, there was no peak in the visible region, but after UV irradiation, two new peaks generated at the visible

region (**Figure 5**). The new peak at 527 nm and 489 nm appeared due to the formation of the covalent organic polymer.

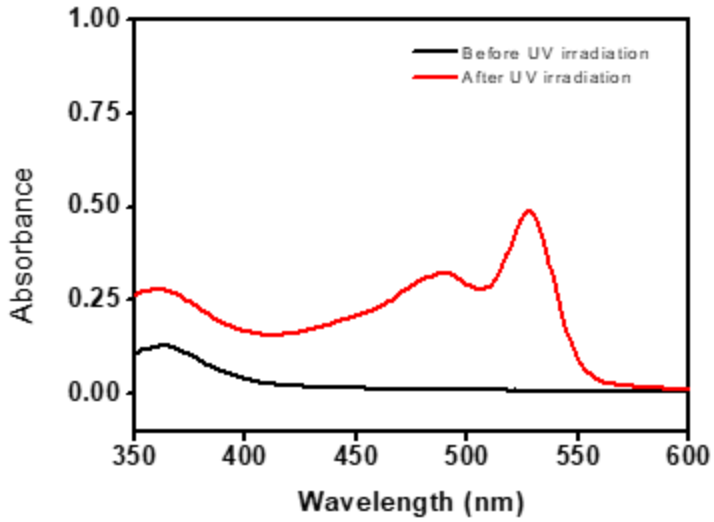

Figure 5. UV-visible spectrum of the compound before and after UV irradiation.

3.5 Raman spectroscopic studies: Raman spectroscopy of the compounds were carried out by using a Jobin Yvon Horiba LABRAM-HR Raman spectrometer. A small amount of powdered sample was taken on a piece of a glass slide, and the spectra were recorded by using a He-Ne laser source having an excitation wavelength of 633 nm and with an acquisition time of 10 seconds using a 10x objective. The compound **8a** prior to the UV irradiation exhibited a peak at 2263 $cm^{-1,}$ which corresponds to the characteristic stretching frequency of 1,3-butadyne. After UV irradiation, we observed the peak at 2263 cm^{-1} diminished, and a new peak at 2102 cm^{-1} appeared (**Figure 6**). The sharp peak at 2102 cm^{-1} was due to the presence of a C≡C bond in the conjugated polymer. From literature, we can say that the peaks between 1400 and 1600 cm^{-1} were due to the stretching vibration of en-yne. The peak at 1490 cm^{-1} was also observed, which is due to the presence of C=C in en-yne conjugated covalent organic polymer.

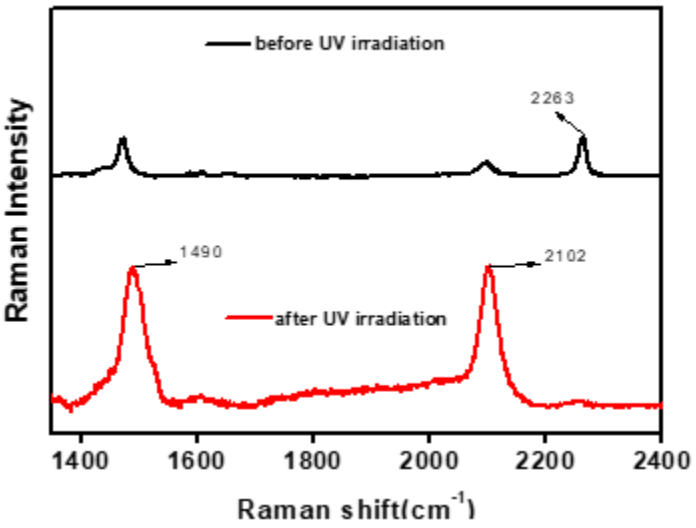

Figure 6. Raman spectrum of the compound before UV irradiation and after UV irradiation.

3.6 Powder X-ray diffraction studies: Powder X-ray diffraction studies were carried out by putting the samples on the glass plate. Experiments were recorded using Rigaku Smart Lab X-ray diffractometer with a wavelength of 1.5406 Å. To know the structural information, compound **8a** was characterized by powder X-ray diffraction (PXRD) technique. PXRD spectra of both before UV irradiation and after UV irradiation shows strong diffraction lines around $2\Theta = 20^{o}$ (**Figure 7**). There are no significant changes in PXRD spectra of compound **8a** before UV irradiation and after UV irradiation. The diffraction peak at $2\theta = 20.12^{\circ}$ (d = 4.4Å) at $2\theta = 21.33^{\circ}$ (d = 4.16Å) were the characteristic distance between hydrogen-bonded two molecules. The specific π-π stacking interactions between the aromatic motifs played a significant role during the self-assembly, which was revealed from the diffraction peak at $2\theta = 28.74^{\circ}$ corresponding to the d spacing value 3.10Å.

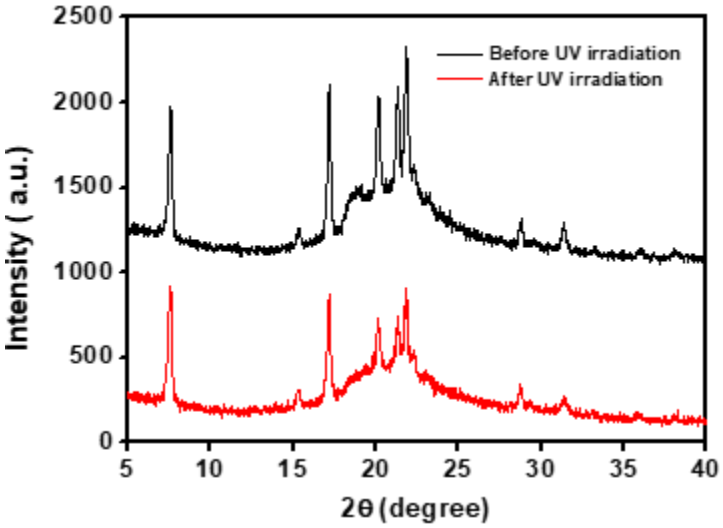

Figure 7. Wide angle powder X-ray diffraction spectrum of the compound 8a before and after UV light irradiation.

3.7 Morphological studies: We examined the morphologies of the toluene gels of compound 8a before and after UV irradiation by SEM (Scanning Electron Microscopy) images. SEM images of xerogel of compound 8a showed like cross-linked fibrous network before (**Figure 8a**) and after UV irradiation (**Figure 8b**). No significant morphological change was observed after the photopolymerization.

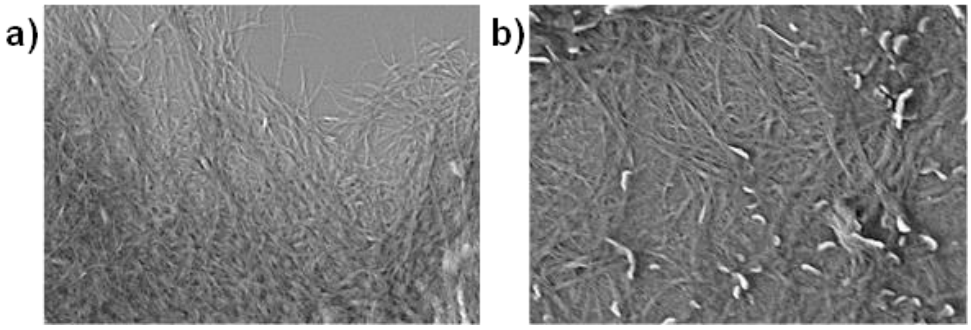

Figure 8. SEM images of the compound a) before UV irradiation, b) after UV irradiation.

For the morphological studies, Atomic Force Microscopy (AFM) was also performed of the gels of compound **8a** before and after UV irradiation. AFM images also show the fibrous network before (**Figure 9a**) and after (**figure 9b**)

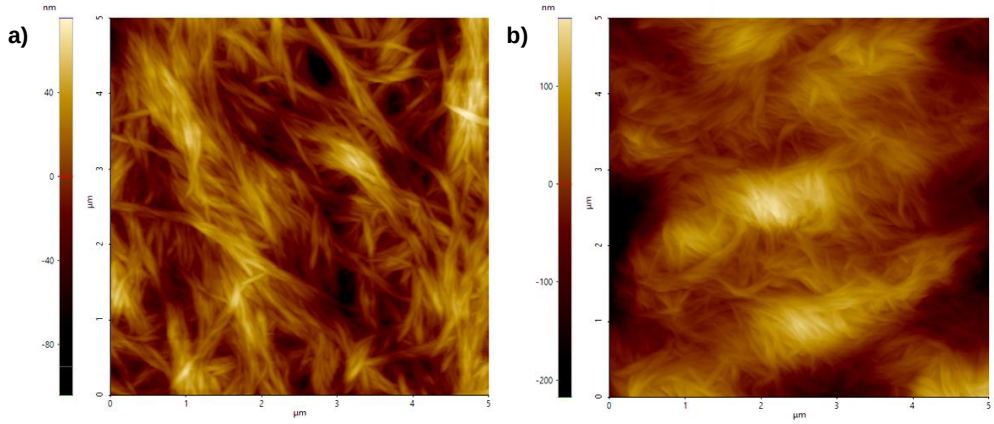

UV irradiation. Both before UV irradiation and after UV irradiation shows similar kind of morphology.

Figure 9 AFM images of the compound a) Before UV irradiation b) After UV irradiation.

3.8 Cyclic voltammetry (CV) studies: The electrochemical measurement was performed in a single cell of three electrodes. The working electrode was prepared by drop-casting the solution (1 mg/mL in tetrahydrofuran) of polymer sample on glassy carbon (GC) electrode, a Pt wire was used as a counter electrode, and the reference electrode was Ag/AgCl. The working electrode was dipped into the electrochemical cell, which contains 0.1 M tetrabutylammonium hexafluorophosphate ($TBAPF_6$) solution in acetonitrile. The cyclic voltammetry experiment of the compound was performed from the range of −3.0 V to +3.0 V. The CV measurement shows that the oxidation and reduction processes of the covalent organic polymers are irreversible. From the cyclic voltammogram of covalent organic polymer it was observed that the oxidation peak at +1.7 V and the reduction peak at -0.9 V (**Figure 10**) and the calculated band gap of the polymer was 2.78 eV. For the calculation of band gap, we have used the following formulas,

$$E_{HOMO} = -[E_{Ox.}^{onset} + 4.8 - E_{ferrocene}]\ eV$$

$$E_{LUMO} = [E_{Red.}^{onset} + 4.8 - E_{ferrocene}]\ eV$$

$$E_{band\ gap} = [E_{LUMO} - E_{HOMO}]\ eV$$

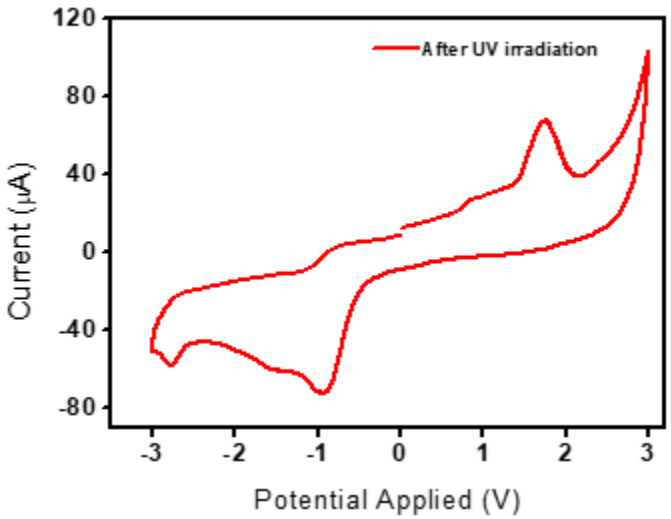

Figure 10. Cyclic voltammogram of PDA-COP0.

3.9 Dye degradation studies: The electronic properties of the covalent organic polymer were investigated to explain the source of the photocatalytic activity in the presence of UV light. Cyclic voltammetry (CV) experiments were performed to determine the band gap of the covalent organic polymer, and it reveals that the band gap was 2.6 eV. This experimental data supports the activity of the covalent organic polymer as a photocatalyst in the presence of ultraviolet light. Photons carrying energy equal to or higher than that of the band gap (2.6 eV) are capable of generating electrons and holes by the excitation of electrons (e^-) from the valence band (VB) to the conduction band (CB) and keeping the holes (h^+) at the valence band (**Figure 12**). The excited electron reacts with atmospheric O_2 and generates highly reactive superoxide radical. The excited holes react with the water molecule and produce O_2. The superoxide radical plays the main role in the degradation of the organic pollutant to the eco-friendly molecules. Photocatalytic degradation of dye was carried out in the presence of argon gas to examine the role of oxygen. The efficiency of the covalent organic polymer for the disintegration of rhodamine-b dye was reduced to some extent. These experimental results signify the role of superoxide radical ($O_2^{-\bullet}$) in the disintegration of dyes. It is observed that the covalent organic polymer which we have synthesized in this project shows photocatalytic activity for the disintegration of rhodamine-b dye in the presence of UV light (**Figure 11a**). The percentage of rhodamine-b dye disintegrates in the presence of the

UV light with the help of covalent organic polymer as a photocatalyst was calculated by using the below-given equation, where A_0 is the absorbance of the dye at the initial stage, and A_t is the absorbance of the dye at a time "t."

$$\% \text{ degradation} = (A_0 - A_t)/A_0$$

By using this equation, it is observed that after the120 minutes irradiation of UV light Photocatalyst (COP) was able to degrade 87% of the rhodamine-b dye. The covalent organic polymer was found to be highly stable, and there was no significant weight loss observed after several photocatalytic reactions. The stability of the photocatalyst was explained by the given FT-IR spectrum, which shows no significant change prior and later to the photocatalysis (**Figure 11b**).

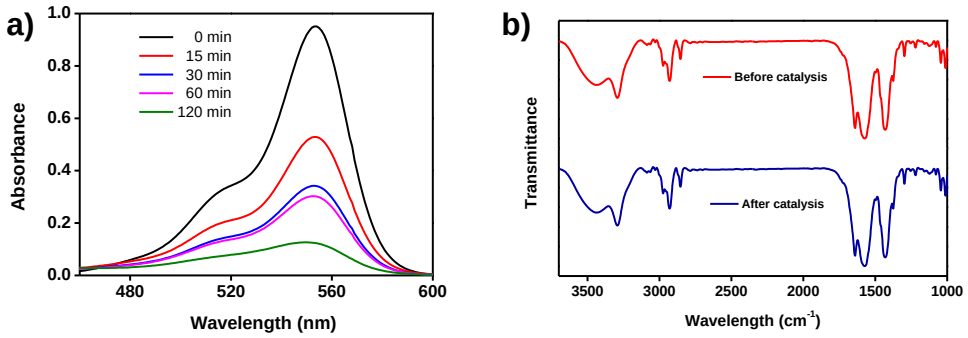

Figure 11. a) Photocatalytic degradation of rhodamine b dye in the presence of PDA-COP under UV light, b) FT-IR spectrum of the compound before and after catalysis.

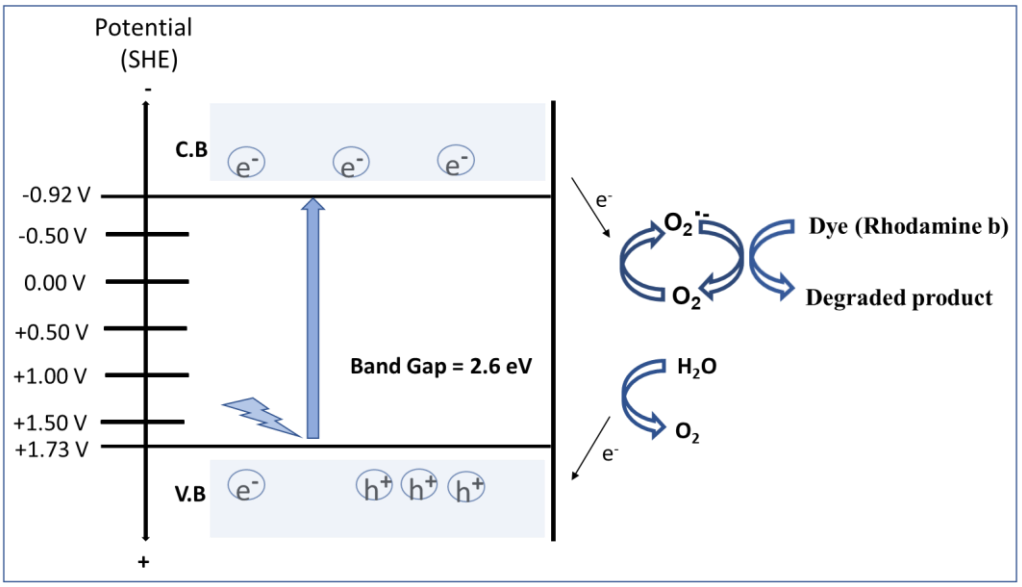

Figure 12. A probable mechanism for dye degradation in the presence of COP as a photocatalyst.

Chapter 4: Conclusion

We have synthesized and characterized a peptide-containing diacetylene based compound. Further, we have studied the topochemical photopolymerization of this compound and also the gelation test. The compound showing gelation properties in the toluene solvent and it undergoes photopolymerization readily under UV light exposure to form conjugated ene-yne based covalent organic polymer (COP). The covalent organic polymer exhibits photocatalytic activity and degrades rhodamine b upon the treatment of UV light.

APPENDIX-A

^{1}H NMR, ^{13}C NMR and Mass Spectrometry of the compounds

Figure 13: ^{1}H NMR (400 MHz, $CDCl_3$) spectrum of compound **4a:**

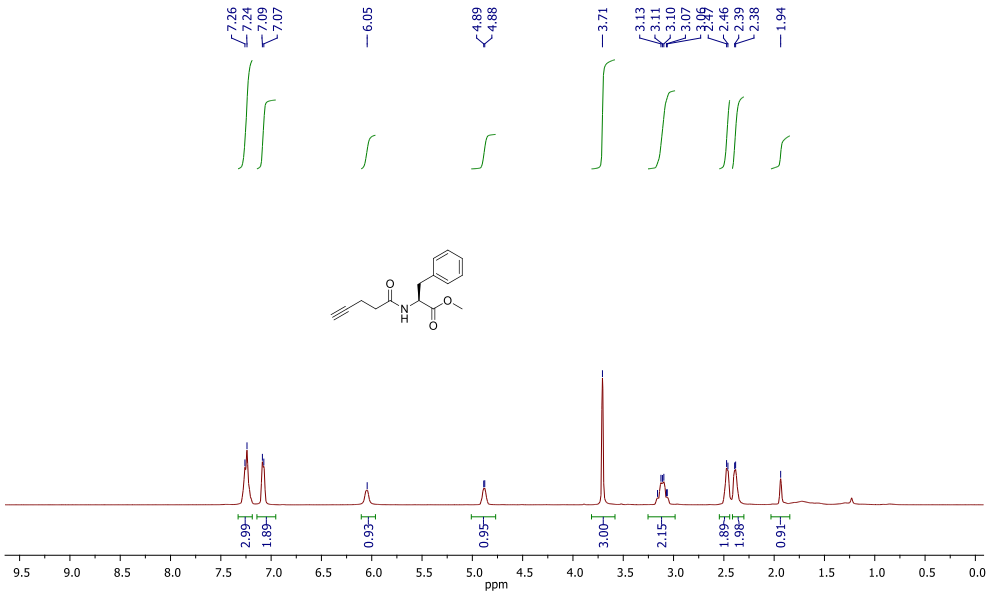

Figure 14: ^{13}C NMR (100 MHz, $CDCl_3$) spectrum of compound **4a**:

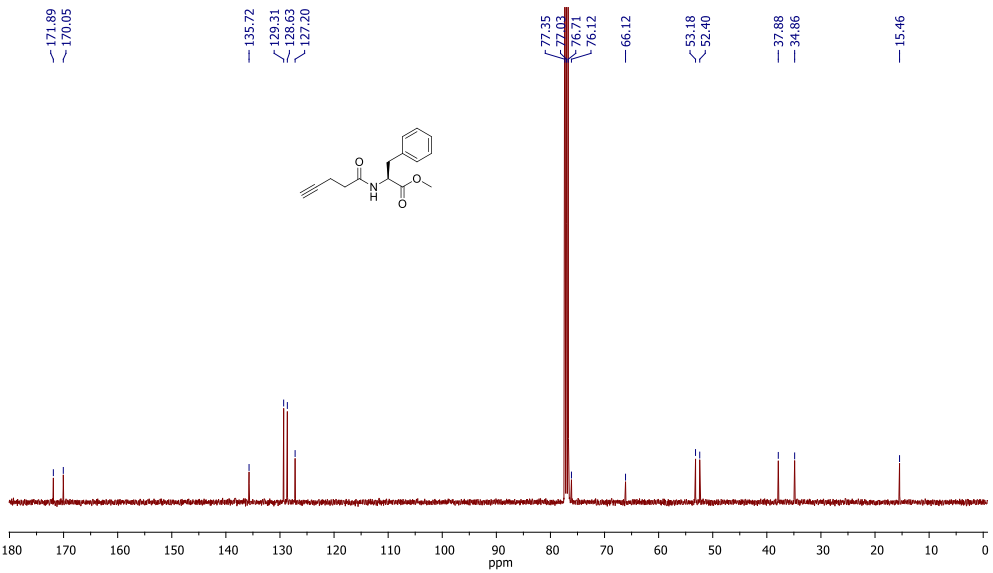

Figure 15: ^{1}H NMR (400 MHz, $CDCl_3$) spectrum of compound **5a**:

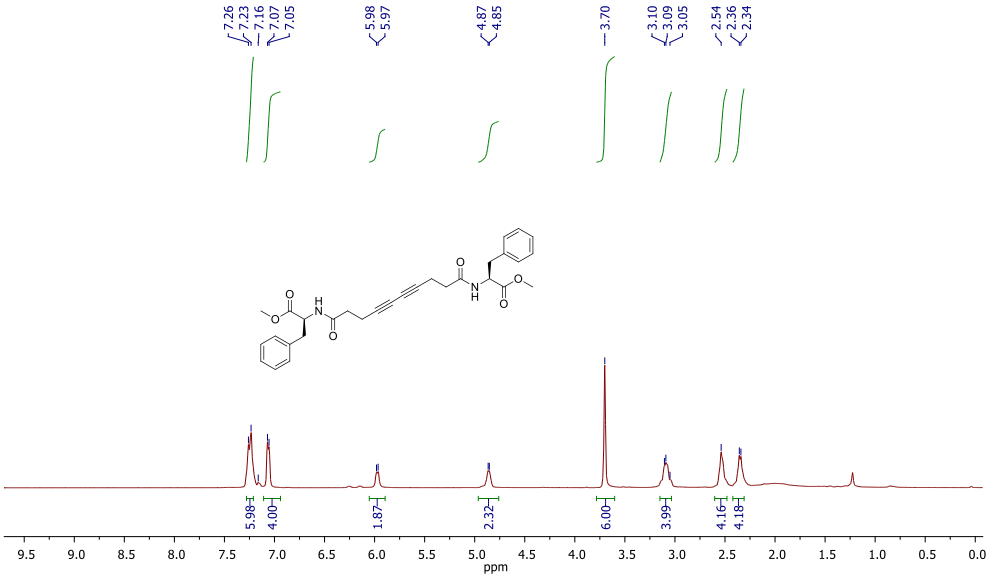

Figure 16: ^{13}C NMR (100 MHz, $CDCl_3$) spectrum of compound **5a**:

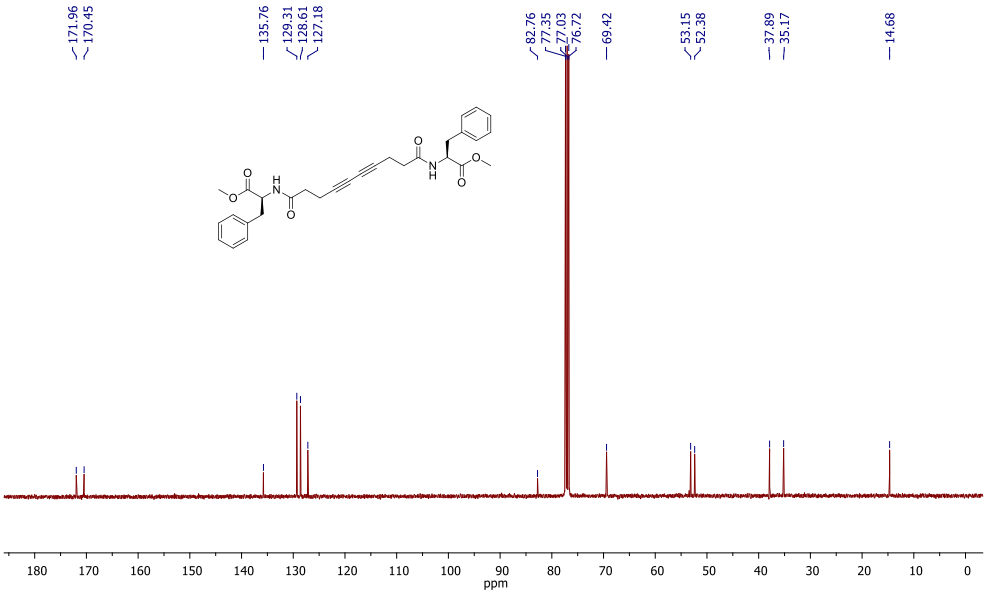

Figure 17: ^{1}H NMR (400 MHz, DMSO-d_6) spectrum of compound **6a**:

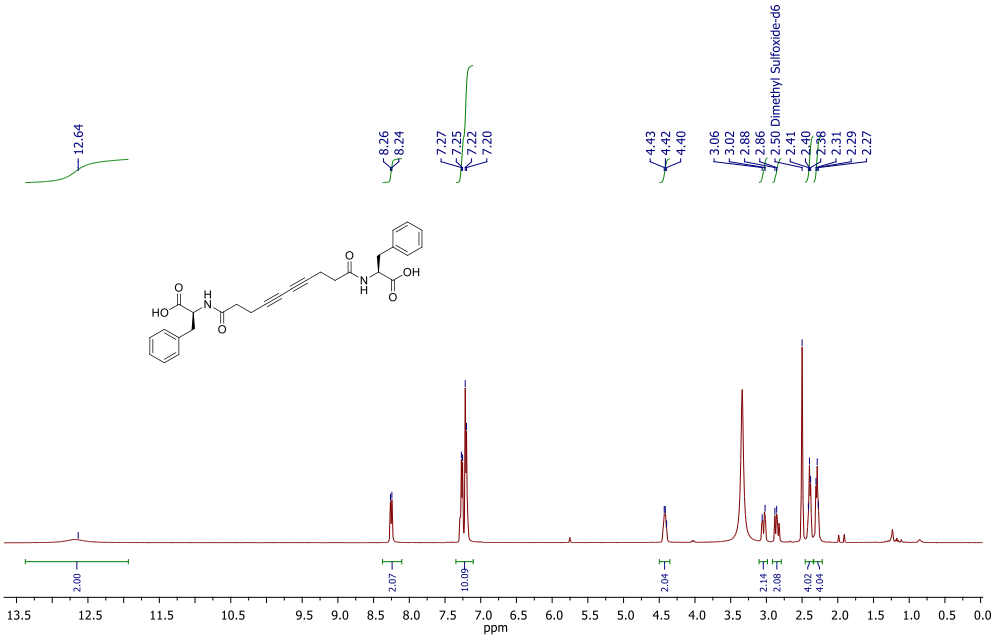

Figure 18: ^{13}C NMR (100 MHz, DMSO-d_6) spectrum of compound **6a**:

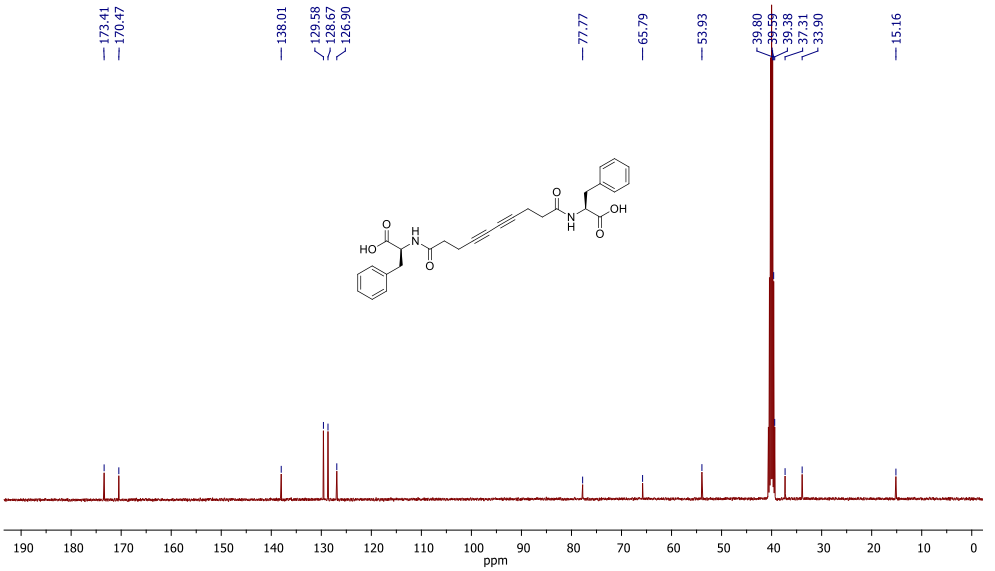

Figure 19: ^{1}H NMR (400 MHz, DMSO-d_6) spectrum of compound **8a**:

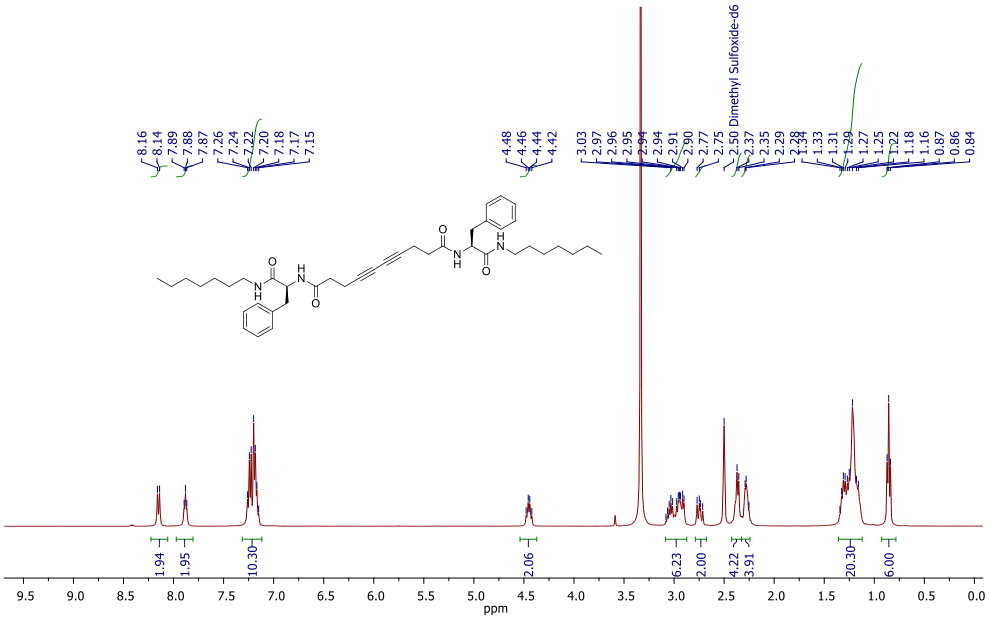

Figure 20: ^{13}C NMR (100 MHz, DMSO-d_6) spectrum of compound **8a**:

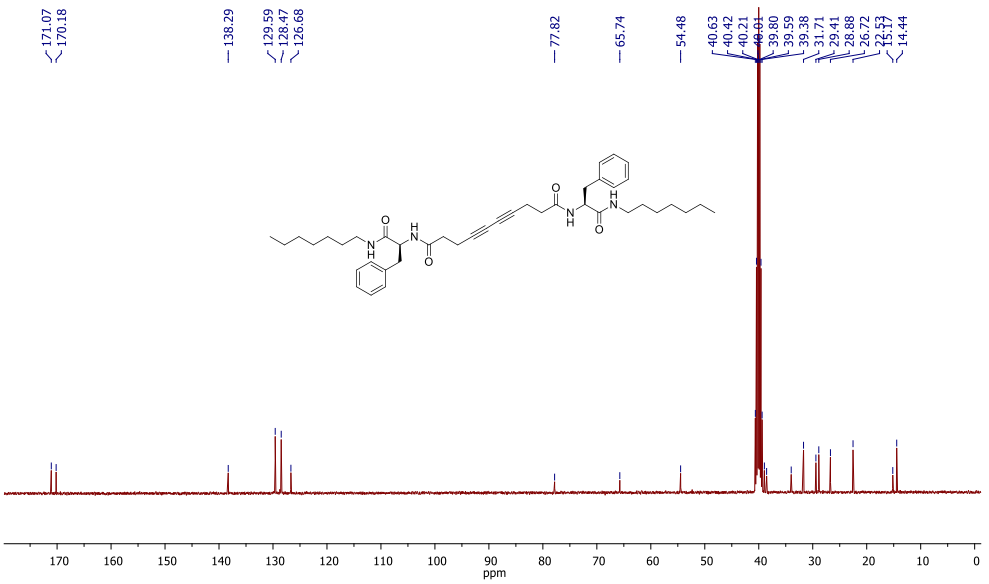

Figure 21: ESI-MS spectrum of compound **4a:**

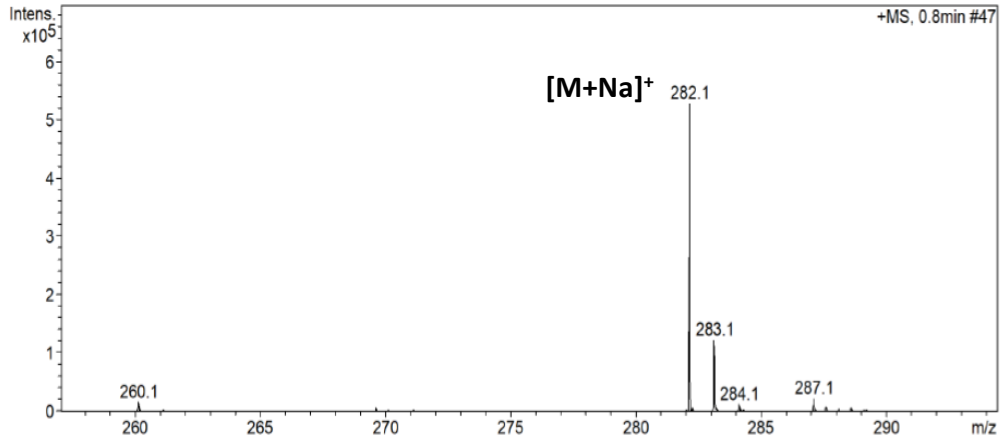

Figure 22: ESI-MS spectrum of compound **5a:**

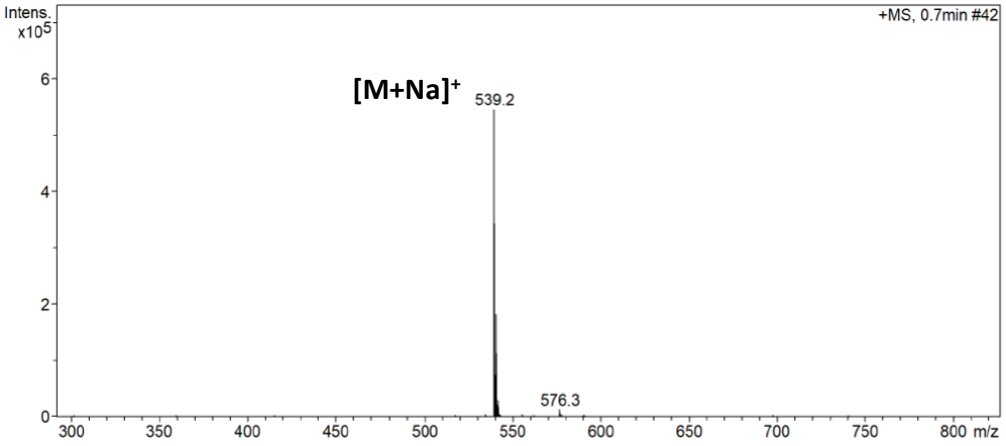

Figure 23: ESI-MS spectrum of compound **6a:**

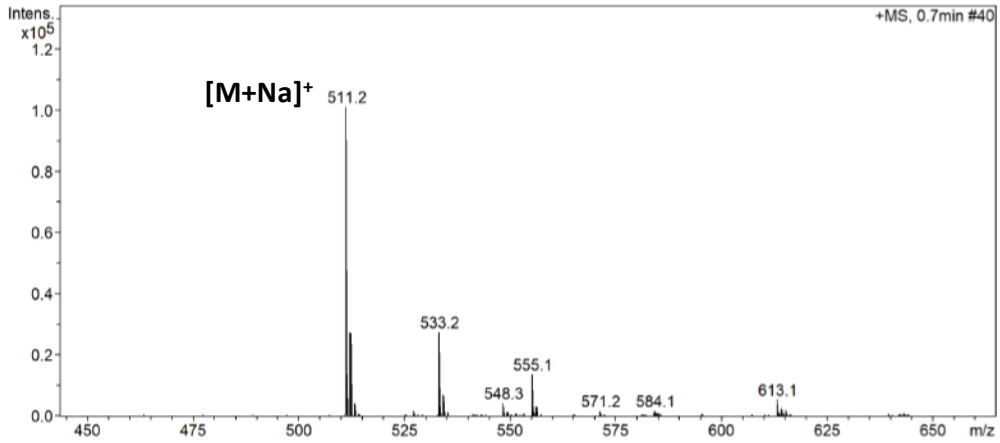

Figure 24: ESI-MS spectrum of compound **8a:**

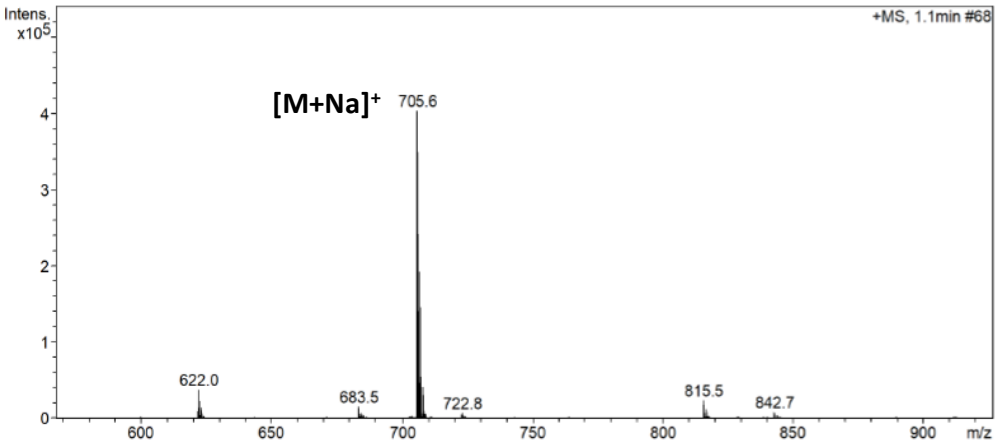

REFERENCES

1. Zhang Y. Q., Yang X. B., Wang Z. X., Long J., Shao L. (2017). Designing multifunctional 3D magnetic foam for effective insoluble oil separation and rapid selective dye removal for use in wastewater remediation. *Journal of Materials Chemistry A*, **5(16)**, 7316-7325.
2. Jelinek R., & Ritenberg M. (2013), Polydiacetylenes–recent molecular advances and applications. *RSC Advances*, **3(44)**, 21192-21201.
3. Li G., Zhang K., Tsuru T. (2017), Two-Dimensional Covalent Organic Framework (COF) Membranes Fabricated via the Assembly of Exfoliated COF Nanosheets, *ACS Appl. Mater. Interfaces* **9**, 8433−8436.
4. Diercks C. S., Yaghi O. M. (2017), The Atom, the Molecule, and the Covalent Organic Framework, *Science*, **355**, eaal1585.
5. Zha Z., Xu L., Wang Z., Li X., Pan Q., Hu P., Lei S. (2015), 3D Graphene Functionalized by Covalent Organic Framework Thin Film as Capacitive Electrode in Alkaline Media, *ACS Appl. Mater. Interfaces*, **7**, 17837−17843.
6. Medina D. D., Werner V., Auras F., Tautz R., Dogru M., Schuster J., Linke S., Döblinger M., Feldmann J., Knochel P., Bein T. (2014), Oriented Thin Films of a Benzodithiophene Covalent Organic Framework, *ACS Nano*, **8**, 4042−4052.
7. Krishnan B. P., Mukherjee S., Aneesh P. M., Namboothiry M. A., Sureshan K. M. (2016), Semiconducting fabrics by in situ topochemical synthesis of polydiacetylene: A new dimension to the use of organogels. *Angewandte Chemie International Edition*, **55(7)**, 2345-2349.
8. Liu D., Wu Z., Tian F., Ye B. C., Tong Y. (2016), Synthesis of N and La Co-Doped TiO2/AC Photocatalyst by Microwave Irradiation for the Photocatalytic Degradation of Naphthalene, *J. Alloys Compd.*, **676**, 489−498.
9. Chidambaram S., Pari B., Kasi N., Muthusamy S. (2016), ZnO/Ag Heterostructures Embedded in Fe3O4 Nanoparticles for Magnetically Recoverable Photocatalysis, *J. Alloys Compd.*, **665**, 404−410.
10. Liu Y., Yu L., Hu Y., Guo C., Zhang F., Lou X. W. D. (2012), A Magnetically Separable Photocatalyst Based on Nest-like γ-Fe2O3/ ZnO Double-Shelled Hollow Structures with Enhanced Photocatalytic Activity, *Nanoscale*, **4**, 183−187.
11. Ansari S. A., Khan M. M., Ansari M. O., Lee J., Cho M. H. (2013), Biogenic Synthesis, Photocatalytic, and Photoelectrochemical Performance of Ag−ZnO Nanocomposite, *J. Phys. Chem. C*, **117**, 27023− 27030.

12. Hoffmann M. R., Martin S. T., Choi W., Bahnemann D. W. (1995), Environmental Applications of Semiconductor Photocatalysis, *Chem. Rev.*, **95**, 69−96.
13. Wang X. H., Li J. G., Kamiyama H., Moriyoshi Y., Ishigaki T. (2006), Wavelength-Sensitive Photocatalytic Degradation of Methyl Orange in Aqueous Suspension over Iron(III)-Doped TiO_2 Nanopowders under UV and Visible Light Irradiation, *J. Phys. Chem. B*, **110**, 6804− 6809.
14. Yu J. C., Yu J., Ho W., Jiang Z., Zhang L. (2002), Effects of F-Doping on the Photocatalytic Activity and Microstructures of Nanocrystalline TiO2 Powders. *Chem. Mater.*, **14**, 3808−3816.
15. Hernández-Alonso M. D., Fresno F., Suárez S., Coronado J. M. (2009), Development of Alternative Photocatalysts to TiO2: Challenges and Opportunities. *Energy Environ. Sci.*, **2**, 1231−1257.
16. Wang M., Ioccozia J., Sun L., Lin C., Lin Z. (2014), Inorganic- Modified Semiconductor TiO2 Nanotube Arrays for Photocatalysis. *Energy Environ. Sci.*, **7**, 2182−2202.
17. Zhang Z., Wang C. C., Zakaria R., Ying J. Y. (1998), Role of Particle Size in Nanocrystalline TiO_2-Based Photocatalysts. *J. Phys. Chem. B*, **102**, 10871−10878.
18. Ji H., Huang Z., Xia Z., Molokeev M. S., Atuchin V. V., Fang M., Huang S. (2014), New Yellow-Emitting Whitlockite-Type Structure $Sr_{1.75}Ca_{1.25}(PO_4)_2:Eu^{2+}$ Phosphor for Near-UV Pumped White Light-Emitting Devices, *Inorg. Chem.*, **53**, 5129−5135.
19. Li W., Li D., Xian J., Chen W., Hu Y., Shao Y., Fu X. (2010), Specific Analyses of the Active Species on $Zn_{0.28}Cd_{0.72}S$ and TiO_2 Photocatalysts in the Degradation of Methyl Orange, *J. Phys. Chem. C*, **114**, 21482−21492.
20. Marschall R. (2014), Semiconductor Composites: Strategies for Enhancing Charge Carrier Separation to Improve Photocatalytic Activity, *Adv. Funct. Mater.*, **24**, 2421−2440.
21. Wang Z., Yang C., Lin T., Yin H., Chen P., Wan D., Xu F., Huang F., Lin J., Xie X., Jiang M. (2013), H-Doped Black Titania with Very High Solar Absorption and Excellent Photocatalysis Enhanced by Localized Surface Plasmon Resonance, *Adv. Funct. Mater.*, **23**, 5444−5450.
22. Wang W. Z., Li W. F., Pan X. Y., Li C. M., Li L. J., Mu Y. G., Rogers J. A., Chan-Park M. B. (2011), Degradable Conjugated Polymers: Synthesis and Applications in Enrichment of Semiconducting Single-Walled Carbon Nanotubes. *Adv. Funct. Mater.*, **21**, 1643−1651.
23. Liu H., Liu H. (2017), Selective Dye Adsorption and Metal Ion Detection Using Multifunctional Silsesquioxane-Based Tetraphenylethene-Linked Nanoporous Polymers. *J. Mater. Chem. A*, **5**, 9156−9162.
24. Laurier K. G. M., Vermoortele F., Ameloot R., De Vos D. E., Hofkens J., Roeffaers M. B. J. (2013), Iron(III)-Based Metal−Organic

Frameworks As Visible Light Photocatalysts. *J. Am. Chem. Soc.*, **135**, 14488−14491.

25. Mao J., Ge M., Huang J., Lai Y., Lin C., Zhang K., Meng K., Tang Y. (2017), Constructing Multifunctional MOF@rGO Hydro-/Aerogels by the Self-Assembly Process for Customized Water Remediation. *J. Mater. Chem. A*, **5**, 11873−11881.
26. Fan K., Nie W. X., Wang L. P., Liao C. H., Bao S. S., Zheng L. M. (2017), Defective Metal−Organic Frameworks Incorporating Iridium-Based Metalloligands: Sorption and Dye Degradation Properties. *Chem. - Eur. J.*, **23**, 6615−6624.
27. Zhao H., Xia Q., Xing H., Chen D., Wang H. (2017), Construction of Pillared-Layer MOF as Efficient Visible-Light Photocatalysts for Aqueous Cr(VI) Reduction and Dye Degradation. *ACS Sustainable Chem. Eng.*, **5**, 4449−4456.
28. Bhowmik S., Jadhav R. G., Das, A. K. (2017), Nanoporous Conducting Covalent Organic Polymer (COP) Nanostructures as Metal-Free High Performance Visible-Light Photocatalyst for Water Treatment and Enhanced CO_2 Capture. *The Journal of Physical Chemistry C*, **122(1)**, 274-284.
29. Ghosh S., Kouamé N. A., Ramos L., Remita S., Dazzi A., et. al. (2015). Conducting polymer nanostructures for photocatalysis under visible light. *Nature materials*, **14(5)**, 505.
30. Bhowmik S., Konda M., Das A. K. (2017), Light induced construction of porous covalent organic polymeric networks for significant enhancement of CO_2 gas sorption. *RSC Advances*, **7(75)**, 47695-47703.